IEEE Photonics Journal
An IEEE Photonics Society Publication

Open Access

A New RAM Normalized 1*f*-WMS Technique for the Measurement of Gas Parameters in Harsh Environments and a Comparison With 2*f*/1*f*

Volume 10, Number 6, December 2018

Abhishek Upadhyay
Michael Lengden
David Wilson
Gordon Samuel Humphries
Andrew P. Crayford
Daniel G. Pugh
Mark P. Johnson
George Stewart
Walter Johnstone

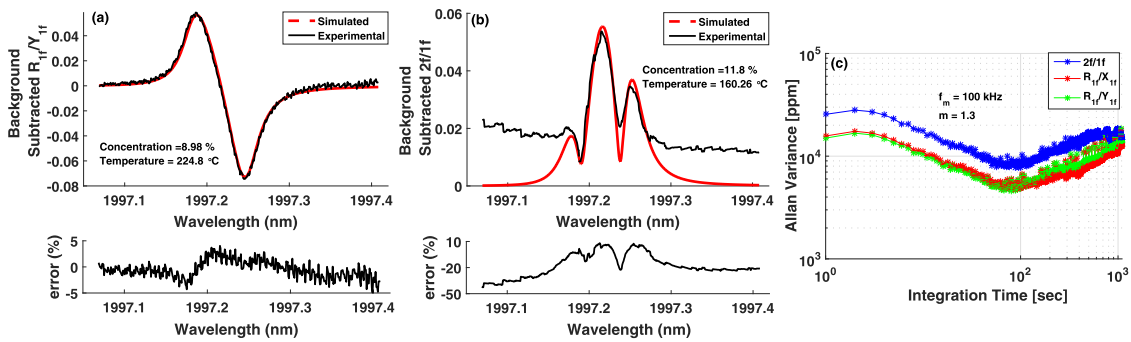

DOI: 10.1109/JPHOT.2018.2883548

A New RAM Normalized 1*f*-WMS Technique for the Measurement of Gas Parameters in Harsh Environments and a Comparison With 2*f*/1*f*

Abhishek Upadhyay,[1] **Michael Lengden**,[1] **David Wilson**,[1] **Gordon Samuel Humphries**,[1] **Andrew P. Crayford**,[2] **Daniel G. Pugh**,[2] **Mark P. Johnson**,[3] **George Stewart**,[1] **and Walter Johnstone**[1]

[1]Centre for Microsystems and Photonics, Electrical and Electronics Engineering Department, University of Strathclyde, Glasgow G1 1RD U.K.
[2]Gas Turbine Research Centre, Cardiff School of Engineering, Cardiff University, Cardiff CF10 3AT, U.K.
[3]Rolls-Royce plc., Derby DE24 8BJ, U.K.

DOI:10.1109/JPHOT.2018.2883548

Manuscript received September 8, 2018; revised October 26, 2018; accepted November 21, 2018. Date of publication November 27, 2018; date of current version December 10, 2018. This work was supported in part by the Fibre-Laser Imaging of Gas Turbine Exhaust Species project, EPSRC, under Grant EP/J002178/1 and in part by the In-situ Chemical Measurement and Imaging Diagnostics for Energy Process Engineering project, EPSRC, under Grant EP/P001661/1. Corresponding author: Abhishek Upadhyay (e-mail: abhishek4u.jss@gmail.com).

Abstract: A calibration-free first harmonic (1*f*) wavelength modulation spectroscopy (1*f*-WMS) technique for gas species parameter measurement is demonstrated. In this technique, the total magnitude of the 1*f*-WMS signal is normalized by a component of the 1*f* residual amplitude modulation signal. This method preserves the advantages of the traditional *nf*/1*f*-WMS ($n \geq 2$) technique, such as the immunity to the non-absorbing systematic losses and the accurate recovery of gas parameters, without the requirement for non-absorbing regions for normalization at high pressure or high modulation index values (*m*-values). The proposed technique only requires the 1*f* signal, which has the largest magnitude of all the harmonics signals, and, therefore, fundamentally has a higher sensitivity to the *nf*/1*f* technique. Furthermore, since only the 1*f*-WMS signal is used, the technique is less complex in terms of signal processing and data acquisition. This paper also shows a comparison of the proposed technique and 2*f*/1*f* for measuring CO_2 in the exhaust of a combuster. The data highlight how nonlinearities in the optical detection system as a function of frequency have a considerable effect on the recovered 2*f*/1*f* spectra, causing variation in the recovered gas concentrations. This effect is not seen in the methodology proposed in this paper.

Index Terms: Wavelength modulation spectroscopy, Calibration-free TDLS, 1*f*-WMS.

1. Introduction

In many environments, such as in combustion measurements, there are significant variations in the measured signal that are not due to the variation of the gas parameters but are due to the presence of significant optical beam steering and mechanical vibrations in the system. In such environments it is often very difficult to account for these variations through a calibration step, especially if periodic recalibration is not a viable solution due to limited post installation access. To overcome this

issue a number of 'calibration-free' tunable diode laser spectroscopy with wavelength modulation (CF-WMS) techniques have been developed over the last two decades that do not require a reference measurement of the laser's optical intensity [1]–[6]. As with all WMS methodologies, the CF-WMS techniques require a dual current modulation to be applied to the gas interrogation laser; the first current modulation is a low frequency ramp or sinusoidal waveform that wavelength tunes the laser over the spectral absorption feature of interest, the second is a high frequency sinusoidal waveform ($\omega_m = 2\pi f_m$) that provides higher detection sensitivity through the use of phase-sensitive detection, typically using a lock-in amplifier (LIA), and thus shifting the signal to the base-band. The high frequency current modulation applied to the laser results in an output intensity modulation (ΔI), known as the Residual Amplitude Modulation (RAM), and a phase delayed wavelength modulation (WM), that both interact with the gas to generate harmonic signals that relate to the optical absorption. Of particular interest in CF-WMS is the direct RAM signal output from the laser, which results in a large DC output from the 1st harmonic of the LIA that can be used for normalisation of WMS signals.

One of the first CF-WMS approaches, known as the 1*f*-RAM technique, recovers the in-phase and quadrature signals from a LIA at the fundamental modulation frequency, f_m. [2], [3], [7], [8], when the LIA phase is preset to isolate the generated 1*f*-RAM components, from the phase delayed WM components. In this case, the isolated 1*f*-RAM component is similar to the absolute gas absorption line-shape, allowing the recovery of gas parameters in the same manner as using direct tunable diode laser spectroscopy. However, this approach has had limited success, as it only utilises the RAM component of the recovered first harmonic signal rather than the total magnitude, and therefore the overall sensitivity of this approach is reduced. Furthermore, the 1*f*-RAM component still contains the DC offset that is proportional to the ΔI output from the laser, which still requires normalisation. Although this normalisation can be achieved using an off-line ΔI measurement or by fitting a polynomial to the non-absorbing regions of RAM signal it does not compensate for significant optical fluctuations prevalent in harsh environments.

A more suitable CF-TDLS methodology for harsh environments is the *nf*/1*f* technique ($n \geq 2$) [4], [5], [9], [10]. In this approach, the total magnitude of signals are recovered at both f_m and one of the *n*th harmonics, R_{1f} and R_{nf} respectively. In general and as discussed above, the major component of R_{1f} is the 1*f*-RAM component that is proportional to ΔI. At higher harmonics, there is no DC RAM offset, and the major component of R_{nf} signals is the *n*th derivative of the gas absorption line-shape that is directly proportional to the optical intensity, I and also dependent on the wavelength modulation amplitude, $\delta\nu$. Therefore, the division of R_{nf} by R_{1f} results in a signal that is made up of individual components that are dependent on $I/\Delta I$. As this value is a constant for any given laser operating condition the normalized signal becomes immune to optical intensity fluctuations but is still dependent on gas absorption.

A number of issues have to be discussed with regards to the *nf*/1*f* technique. Firstly, if the laser's output intensity is highly non-linear as a function of the drive current then gas independent RAM signals (ΔI_n) begin to appear at higher harmonics, and this has been shown to significantly affect gas measurement recovery at the second harmonic [11]–[13]. Thus further laser characterisation would be required Δi_2, Δi_3, ψ_2 etc within the theoretical model. Secondly, as the magnitude of the recovered harmonic signal reduces as the targeted harmonic increases, the overall sensitivity of the *nf*/1*f* technique will theoretically decrease as compared to 1*f* techniques [9], [10], [13]. Furthermore, as the recovered signals in *nf*/1*f* are at two different frequencies, they will suffer from different pass-band noise that will not be cancelled in the normalisation process. Finally, the required digital sampling rate increases linearly with the targeted harmonic, thus also increasing the overall data transfer rate and data storage requirements for the *nf*/1*f* approach. Although this final point may not be significant for single measurement path systems, it becomes an increasingly difficult problem to manage as the number of required measurement paths increases, for example with chemical species tomography techniques [14] where in excess of 100 simultaneous path-integrated absorption measurements may be recorded.

Considering the above discussion the development of a CF-WMS technique that only requires the recovery of signals at 1*f* with 1*f*-RAM normalisation and utilises the total magnitude of the first

harmonic signal would be highly advantageous, as it provides an improved sensitivity and requires lower associated data and computational complexity. In this paper we demonstrate a CF-1*f*-WMS technique that normalises the R_{1f} signal by an isolated projection of the 1*f*-RAM signal, as described in Section 2. As evidenced in Section 3, the overall sensitivity achieved by this method is better than that achieved using 2*f*/1*f* WMS for carbon dioxide detection. However, it must be noted that the sensitivity comparison in this paper is only for one specific laser and one set of laser operational parameters. A more general sensitivity comparison between the two techniques is not the aim of this paper and would require further research. Finally, we compare this new approach with the 2*f*/1*f* technique directly for path integrated CO_2 concentration and system temperature measurements in the exhaust plume of a combuster located at the gas turbine research center (GTRC) of the University of Cardiff. The two techniques are also compared with extractive CO_2 concentration measurements using a non-dispersive infrared (NDIR) analyzer and temperature measurements obtained with thermocouples. These exhaust plume tests highlighted a number of issues with the *nf*/1*f* CF-WMS techniques, that can be resolved using the new CF-1*f*-WMS technique. These issues are presented and discussed in detail in Section 4.

2. Methodology for the CF-1*f*-WMS Technique

A brief mathematical description of the generation of WMS signals during the laser-gas interaction is provided here. A more detailed discussion is available in the literature [4], [8]–[10], [15]. When the input current of a tunable semiconductor laser is modulated with a high frequency sinusoid superimposed on a low frequency ramp, there is a resulting simultaneous intensity modulation (IM) and wavelength modulation (WM) output from the laser. The instantaneous IM can be described as $I_{in} = I_0 + \Delta I_1 \cos(\omega_m t) + \Delta I_2 \cos(2\omega_m t + \psi_2 - \psi_1)$, where I_0 is the DC laser intensity and ΔI_1 and ΔI_2 are the first and the second order RAM amplitudes respectively. The generated WM is generally expressed in terms of the laser's output frequency as $\nu = \nu_0 + \Delta\nu \cos(\omega_m t - \psi_1)$, where ν_0 is the DC frequency and $\Delta\nu$ is the amplitude of the frequency modulation, and ψ_1 and ψ_2 are the phase difference between the frequency modulation and the first and second order RAM respectively.

The interaction of the modulated light output from the laser and the transfer characteristics of the gas absorption results in the generation of optical signals at the harmonics of the modulation frequency. The Fourier series expansion of the relative transmission after the laser-gas interaction, $\tau(\nu) = \exp[-\alpha(\nu)l]$, where $\alpha(\nu)$ is the probability of absorption and l is the laser-gas interaction length is given by

$$\tau(\nu) = \sum_{n=0}^{\infty} H_n(\nu_0, \Delta\nu) \cos(n(\omega_m t - \psi_1)) \tag{1}$$

where, $H_n(\nu_0, \Delta\nu)$ is the nth Fourier coefficient of the transfer characteristics of the absorption signal.

For the proposed CF-1*f*-WMS technique only the 1*f* signal is required and, in a similar manner to the 1*f*-RAM technique, the LIA in-phase has to be adjusted so that 1*f*-WM component (H_1) is aligned with one of the LIA axes. This isolates the RAM components on the orthogonal axis allowing them to be used for normalisation. Equations (2)–(4) represent the signals generated on the LIA phase and quadrature axes, X_{1f} and Y_{1f} respectively, and the total magnitude of the 1*f*-WMS signal. This is also shown graphically in Fig. 1.

$$X_{1f} = lH_1 + \Delta I_1 \left(H_0 + \frac{H_2}{2}\right) \cos\psi_1 + \Delta I_2 \left(\frac{H_1}{2} + \frac{H_3}{2}\right) \cos\psi_2 \tag{2}$$

$$Y_{1f} = \Delta I_1 \left(H_0 - \frac{H_2}{2}\right) \sin\psi_1 + \Delta I_2 \left(\frac{H_1}{2} - \frac{H_3}{2}\right) \sin\psi_2 \tag{3}$$

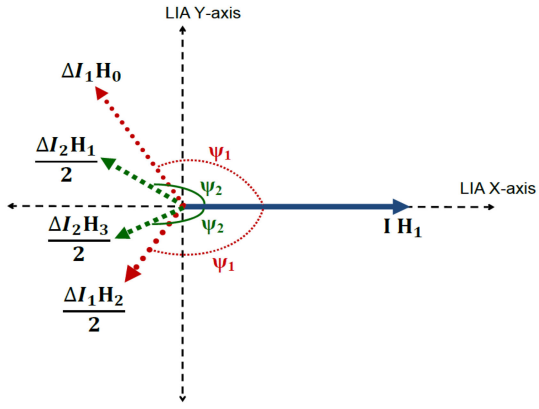

Fig. 1. Phasor representation of first harmonic signal components in the presence of gas.

$$R_{1f} = \sqrt{X_{1f}^2 + Y_{1f}^2} \tag{4}$$

In a similar manner to *nf*/1*f*, we can now divide (4) by (3) to give R_{1f}/Y_{1f}. In this case, we obtain a final signal that is immune to non-absorbing intensity variation caused by mechanical vibration, beam steering, window fouling and light scattering as all the component signals within the ratio are proportional to $(I/\Delta I_1)$, $(I/\Delta I_2)$ or $(\Delta I_1/\Delta I_2)$, which are all assumed to be constant for any given operational characteristic of the laser.

To simulate the R_{1f}/Y_{1f} signal all the laser's operating parameters (I_0, ΔI_1, ΔI_2, ψ_1, ψ_2 and $\Delta\nu$) need to be experimentally obtained, preferably in real time as described previously [13]. I_0 is measured by digital low-pass filtering of the modulated laser output in the absence of gas absorption. As the LIA has been aligned to provide (2) to (4), ψ_n can also be measured in the absence of gas by knowing that

$$\psi_n = \tan^{-1}\left(Y_{nf}/X_{nf}\right) \tag{5}$$

Similarly, the intensity modulation amplitude at all harmonics can be obtained by knowing that

$$\Delta I_n = \left(X_{nf}^2 + Y_{nf}^2\right)^{1/2} \tag{6}$$

In this work $\Delta\nu$ is obtained using a fibre ring resonator [16]. To ensure accurate measurement we have assumed that the fibre ring resonator's free spectral range (FSR) should be at least 10 times smaller than the required $\Delta\nu$ for a modulation index value ($m = \Delta\nu/\gamma$) of 1.3, thus providing at least 10 interferometric peaks for the $\delta\nu$ amplitude measurement. To allow real-time wavelength tuning characterisation we have also assumed that there should be at least 10 samples per interferometric peak, which implies that the sampling rate of the digital data acquisition (DAQ) should be at least 100 times larger than the laser's f_m. It was not possible to measure $\Delta\nu$ in real-time in this work, either in the laboratory validation or the combustor tests, as a high sampling rate DAQ system was not available. Instead, the DC bias of the injection current was varied in small increments and $\Delta\nu$ was obtained for each DC value. However, the methodology to measure $\Delta\nu$ along the entire scan range or at fixed DC bias is the same and has been described previously [10], [13].

3. Experimental Validation of the CF-1*f*-RAM Technique

Fig. 2 shows the experimental set-up used in the laboratory validation of the CF-1*f*-RAM technique. The output of a 2 mW, 1997.215 nm fibre coupled, distributed feedback laser (Eblana Photonics EP1997-DMB01-FM) is passed through a 3-dB optical fibre coupler (Thorlabs 10202A-50-APC). One output from the coupler is connected to a 4 cm long 3D printed gas cell [17] and the other

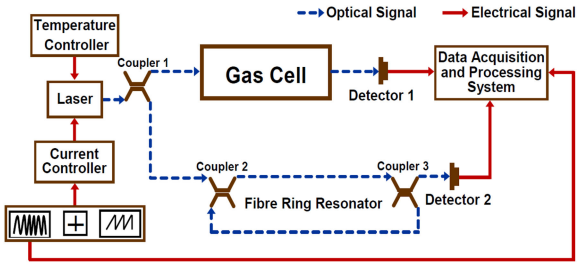

Fig. 2. Schematic of the generic experimental setup used for the implementation of calibration-free 1*f*-WMS technique.

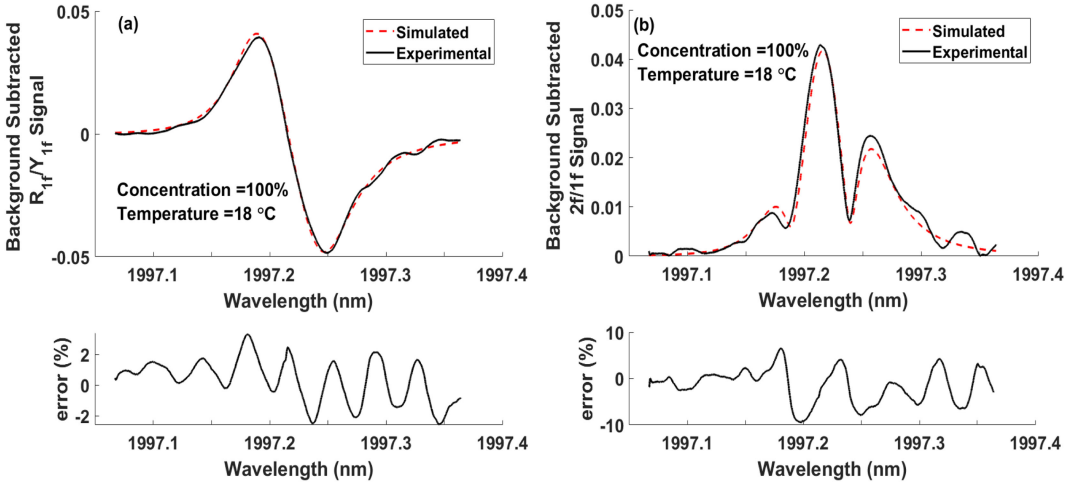

Fig. 3. Magnitude of experimental and simulated (a) R_{1f}/Y_{1f} and (b) $2f/1f$ signals at $m = 1.3$, $f_m = 100$ kHz for 100% carbon dioxide sample at 1 bar pressure and 4 cm optical path length. The corresponding subplots show the percentage error relative to the maximum absorption signal.

output is connected to a fiber ring resonator that has a FSR of 0.4275 GHz. The light transmitted through the gas cell is detected with an extended InGaAs photodetector (Thorlabs PDA10DT-EC) whose output is connected to a National Instruments data acquisition and processing (DAQ) system (Chassis number: PXIe1078, Data Acquisition Card number: PXI6366) that records the raw data output from the receiver. Digital phase sensitive demodulation is then carried out using a custom LabVIEW programme on the PXI host-PC at both the fundamental and second harmonic frequencies. This allows a direct comparison of the proposed technique with $2f/1f$ using the same recorded data. The laser was modulated with a 100 kHz, 24 mA_{pp} sinusoid superimposed on a 10 Hz, 60 mA_{pp} current ramp with an 60 mA central current offset. The m-value in this case is 1.3, maximising the $2f/1f$ signal.

The magnitude of the simulated and experimental R_{1f}/Y_{1f} signals are shown in Fig. 3, for a 100% sample of carbon dioxide at 1 bar. The residual errors have been calculated by measuring the percentage difference between the simulated and experimental signal with the peak to peak signal amplitude being taken as the normalization factor for the background subtracted R_{1f}/Y_{1f} signal and peak amplitude as the normalization signal for the background subtracted $2f/1f$ WMS signal. The residual error for the background subtracted R_{1f}/Y_{1f} signal which is approximately 5% of the maximum absorption signal shows that there is good agreement between the simulated and the experimental signal.

Fig. 4 shows the Allan Variance calculated for both the $2f/1f$ and R_{1f}/Y_{1f} methods using the same recorded data. It also shows the Allan Variance for R_{1f}/X_{1f}, which shows the exact same trend as

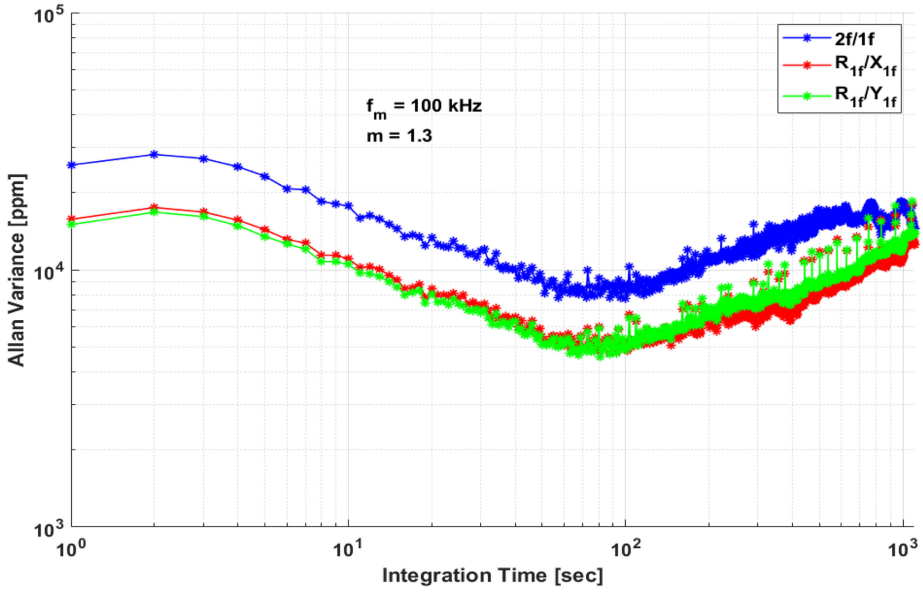

Fig. 4. Allan Variance plot for $2f/1f$, R_{1f}/Y_{1f} and R_{1f}/X_{1f} at $m = 1.3$, $f_m = 100$ kHz for 100% carbon dioxide sample at 1 bar pressure.

R_{1f}/Y_{1f} for this particular set-up. However, we have not carried out a full analysis of the technique to ascertain how the sensitivity is affected by laser modulation characteristics (RAM magnitude, IM/WM phase etc.), lock-in phase or other experimental settings. The concentration sensitivity for the Allan Variance was calculated using a theoretical reference spectral feature modeled using pre-characterized laser parameters to obtain the measured concentration. For a single non-averaged measurement, i.e., the Y-intercept in Fig. 4, it is clear that the $2f/1f$ technique has a lower overall sensitivity compared to the R_{1f}/Y_{1f} method, and this trend continues as a function of the total integration time.

4. Comparison of CF-WMS Methodologies for the In-Situ Measurement of CO_2 in the Exhaust of a Combustor

During the measurement campaign at the Cardiff University's Gas Turbine Research Centre the experimental set-up shown in Fig. 2 was re-configured in two ways. The gas cell was replaced by an 150 mm diameter exhaust duct located 2.15 m downstream from the exhaust of a centrally fired generic diffusion swirl combustor, operated on a Jet A1 fuel, and the extended InGaAs detector was replaced with a mecrury-cadmium-telluride (MCT) detector (Vigo). The light output from the fibre coupled Eblana laser was guided through the duct orthogonally to the direction of the exhaust flow using an aspheric lens fibre collimator (Thorlabs F810APC-2000) via a 3 mm thick, 32 mm diameter MgF_2 window (Crystran Ltd). The light then passed through a second window, located on the opposite side of the duct, prior to detection. As described in Section 3, the data acquisition system recorded the raw data from the photo-receiver, thus allowing different WMS techniques to be compared off-line during the post-processing.

As the laser characterisation data could not be measured in real-time whilst the combustor was in operation, the values of $I/\Delta I_1$ and $I/\Delta I_2$ were obtained throughout the two day testing period at times when the combustor was turned off. Typical spectra obtained using both the R_{1f}/Y_{1f} and $2f/1f$ techniques are shown in Fig. 5. It is clear from this figure that there is significant variation in the ΔI_2 RAM background in the $2f/1f$ data. However, this background variation does not occur in the R_{1f}/Y_{1f} signal, as it is not dependent on the nonlinearity in the optical properties of the system, as

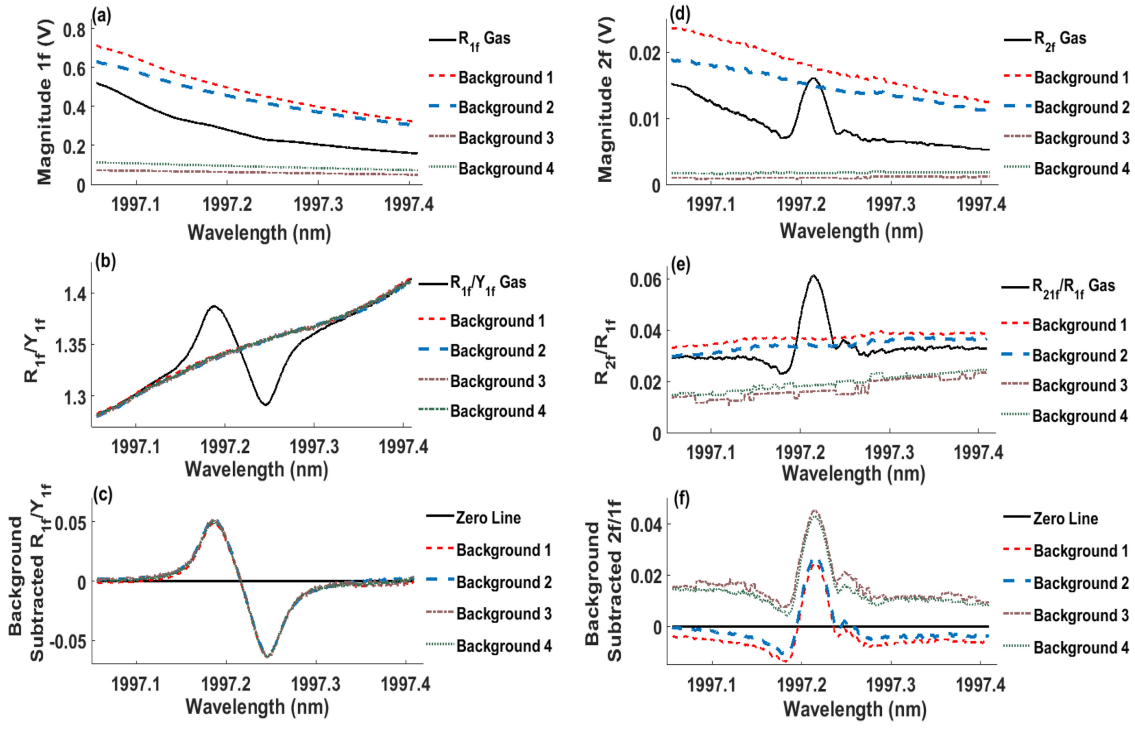

Fig. 5. Comparative spectra obtained using both the R_{1f}/Y_{1f} and $2f/1f$ methodologies for the same measurement data, together with recorded RAM background signals taken at different times during the measurement campaign. Subplots (a) and (d) show the raw 1*f*-WMS and 2f-WMS signal along with their corresponding backgrounds. Subplots (b) and (e) show R_{1f}/Y_{1f} and $2f/1f$ signals taken at the exact same time but processed with background signals taken at various times over the testing period, whereas, subplots (c) and (f) show background subtracted R_{1f}/Y_{1f} and $2f/1f$ signals for each of the corresponding background data.

shown by the equation

$$\frac{R_{1f}^{bkgnd}}{Y_{1f}^{bkgnd}} = \frac{\Delta I_1}{\Delta I_1 \sin(\psi_1)} = \frac{1}{\sin(\psi_1)} \tag{7}$$

Initially, it was assumed that this variation in the ΔI_2 background was caused by significant variation in interferometric noise due to window fouling and mechanical distortion during the combustor testing. However, the majority of this non-linear variation is actually caused by the non-linear behaviour of the MCT output as a function of the detection frequency at high incident optical powers. This is evidenced in Fig. 6 where the lasers $I/\Delta I_1$ characteristics have been measured as a function of incident optical power for both the InGaAs detector and the MCT detector. The data for this figure was acquired by connecting the output fibre from the laser in series with a fibre coupled variable optical attenuator and then a 3 dB optical fibre coupler. One splitter output was then connected directly to the MCT detector and the other splitter output was connected directly to the InGaAs detector. It is clear from Fig. 6 that the $I/\Delta I_1$ characteristics measured using the InGaAs detector remain constant as a function of the optical attenuation. However, in the case of the MCT an attenuation of at least 15 dB is required before the receiver begins to operate in a linear manner at both the DC and 100 kHz modulation frequency. This attenuation corresponds to an incident power on the MCT of 50 μW, and optical powers lower than this value are required in order to obtain accurate laser intensity characterisation.

This non-linear behaviour of the detector causes further difficulties in the WMS signal processing, particularly with the $nf/1f$ technique. In an environment such as a combustor exhaust there is considerable beam steering that causes temporal variation in the incident optical intensity, thus

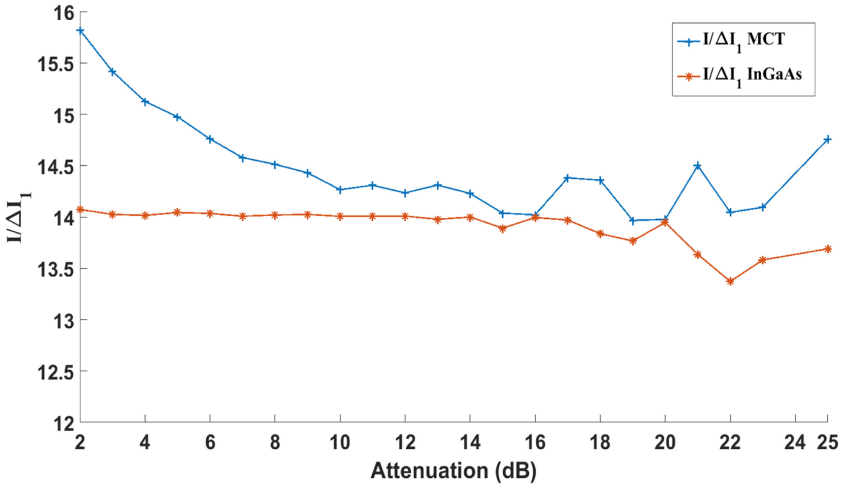

Fig. 6. Variation of the measured $I/\Delta I_1$ at different optical attenuation values for an extended InGaAs photodetector and an Mercury Cadmium Telluride photodetector.

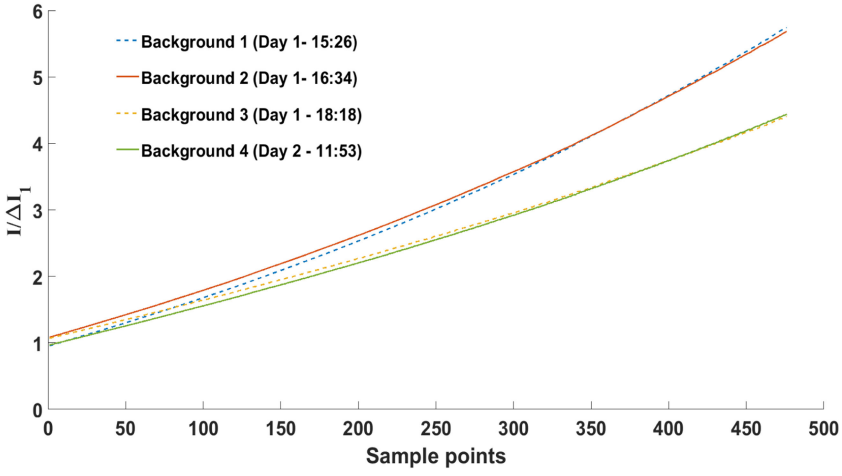

Fig. 7. Variation of the measured $I/\Delta I_1$ using the MCT detector during the Cardiff combustor measurement campaign.

causing temporal variation of the non-linear output of the detector. As shown, this variation in receiver output gain will not have the same effect on the magnitude of the recovered 1f and 2f signals, as the gain varies as a function of input detection frequency. This will lead to significant errors in the recovered 2f/1f signals that cannot be accounted for at any time in the measurement process. Conversely, as the same non-linear gain from the detector affects both the R_{1f} and the Y_{1f} signal by the same magnitude, as they are recovered at the same frequency, any non-linear behaviour of the detector is canceled out in the R_{1f}/Y_{1f} normalisation process, and therefore this technique will still allow accurate modeling and concentration recovery. This non-linear behavior of the detector therefore induces two sources of error in the 2f/1f spectra; the variation in the $\Delta I_2/\Delta I_1$ background that requires subtraction, and more importantly, the detector gain at the 1f and the 2f frequency is not same anymore.

During the Cardiff measurement campaign, the optical power transmitted through the combustor exhaust duct reduced significantly as the optical windows began to collect soot and debris, such that the optical power incident on the MCT reduced to be lower than 50 μW. This allowed accurate measurement of $I/\Delta I_1$ and $I/\Delta I_2$ during the measurement campaign. Fig. 7 shows the measured $I/\Delta I_1$ at different times during the measurement campaign. Background 1 was captured at 15:26

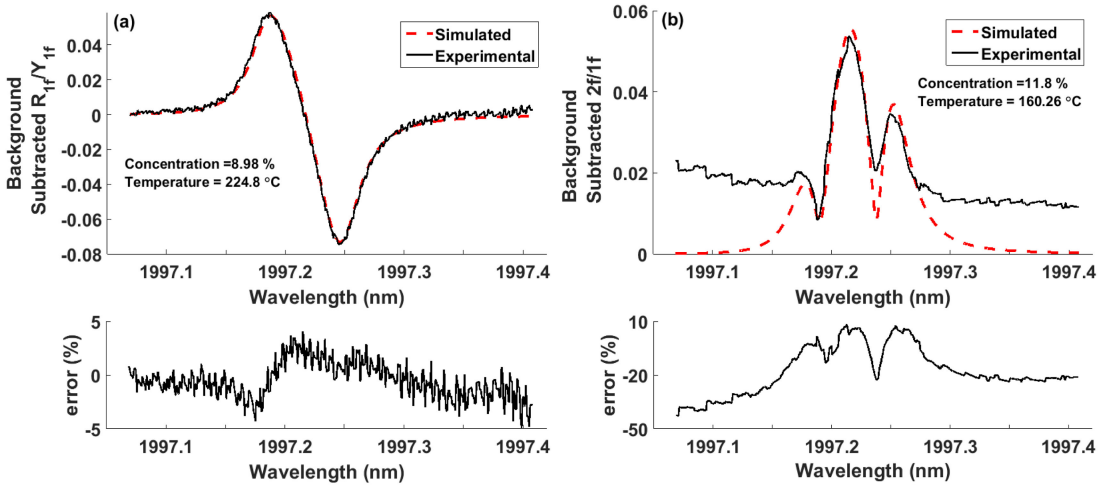

Fig. 8. Comparison of R_{1f}/Y_{1f} and $2f/1f$ for one sample point of the Cardiff measurement campaign. The signals were measured when the MCT was operating in the nonlinear region. However, the laser parameters were measured when the MCT was operating in its linear region (Background 3).

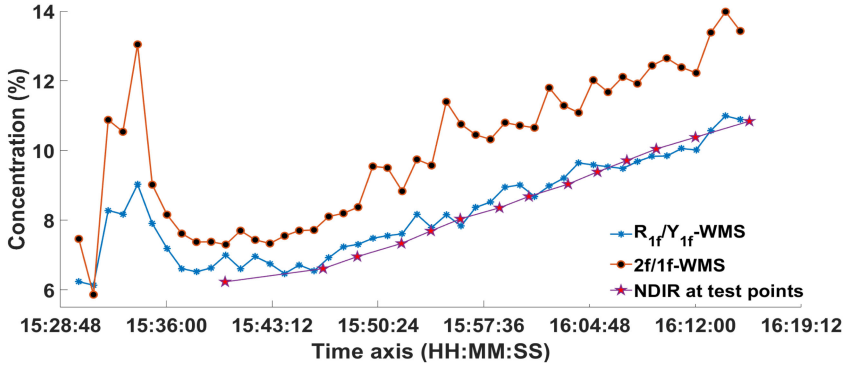

Fig. 9. Comparison of concentration measurements during the Cardiff combustor measurement campaign using R_{1f}/Y_{1f}, $2f/1f$ and NDIR measurement techniques.

(just before the test started) whereas background 2 and 3 were captured after the completion of the test at 16:34 and 18:18 respectively. Background 4 was captured the next day at 11:53. Backgrounds 1 and 2 were in the MCT detector's non-linear operating region where as background 3 and 4 were in the linear region. This was verified using the extended InGaAs detector in the laboratory.

The errors in recovered spectra due to the non-linear output behaviour of the detector is evidenced in Fig. 8, where the two methodologies have been used to calculate the output concentration and temperature. The figure also shows sample experimental data and the associated theoretical fits. In this case, all of the experimental data was obtained when the MCT was behaving non-linearly. However, the laser characterisation data used in the model has been obtained when the detector output is operating in the linear regime. As evidenced, the overall residual error in the fitting of the CF-1*f*-RAM signal is much lower than the error in the $2f/1f$ spectral fitting process.

Finally, comparative data for $2f/1f$ and R_{1f}/Y_{1f} concentration and temperature measurements with gas extractive sampling, and thermocouples located 155 mm upstream and 700 mm downstream of the laser sensor system, are shown in Fig. 9 and 10 respectively. The extractive NDIR gas analyser required the removal of water vapour prior to measurement, providing a 'dry' CO_2 concentration. Therefore, to allow comparison to the measurements made using the two WMS measurement

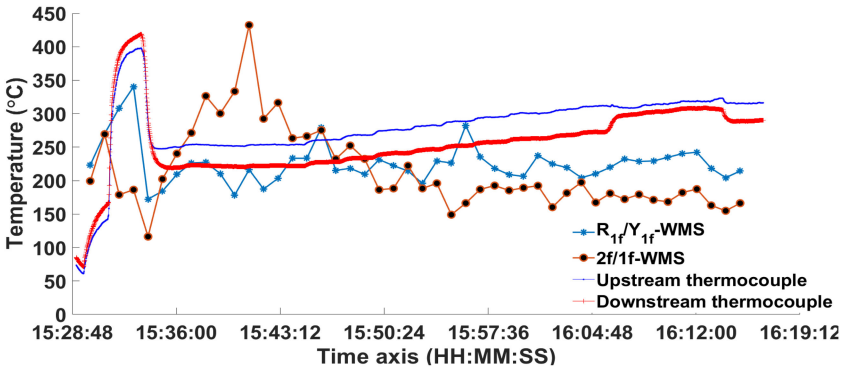

Fig. 10. Comparison of temperature measurements during the Cardiff combustor measurement campaign using R_{1f}/Y_{1f}, $2f/1f$ and the two thermocouples.

techniques, the extractively measured 'dry' concentration was corrected to a wet CO_2 concentration through the simple mass balance of the measured species in the exhaust stream. It is clear that both the concentration measurement WM techniques follow a similar trend to the extractive sampling measurements. However, there is a significant over-estimate in the $2f/1f$ methodology due to the induced errors from the non-linear RAM offset and the non-linearity in the detector gain at the two harmonics. Furthermore, the variation in the background offset causes more variability in the recovered concentration and temperature measurements using $2f/1f$ as compared to the R_{1f}/Y_{1f} technique.

5. Discussion and Conclusion

This is the first demonstration of a calibration-free 1*f*-WMS technique that uses the magnitude of the 1*f*-WMS signal for the measurement of gas parameters. This method is applicable to all types of tunable lasers, both mid-IR and near-IR, operating at any *m*-value. It was verified through Allan variance measurements that show that the minimum sensitivity achieved by the R_{1f}/Y_{1f} method is an improvement on the $2f/1f$ method. However, this has only been verified for the laser parameters required for one particular testing regime, and using one laser and therefore one set of laser modulation characteristics. A more detailed comparison of this technique and other CF-WMS techniques for different laser operating characteristics as well as for different types of lasers is being done at present and the results would be reported in a future publication. The minimum sampling rate required for the R_{1f}/Y_{1f} measurement is half of that required for the corresponding $2f/1f$ measurement. Also, if an embedded system is used for the $2f/1f$ measurement, as compared to R_{1f}/Y_{1f} measurement technique, the requirements in terms of the memory and the processing speed of the embedded system would also be higher. This is due to the necessity to acquire a larger number of signals in the $2f/1f$ technique. We have also shown a comparison of the two techniques during exhaust measurements from a combustor to measure CO_2. In this case, the optical detector showed significant non-linearity as a function of the frequency of the incident optical signal. This non-linearity caused variation in the $2f/1f$ background that could not be compensated for in the signal processing, and also caused distortion in the processed $2f/1f$ data due to the gain variation in the first and second harmonic signals. Neither of these drawbacks are present in the technique proposed in this work, as the background signal just depends on the ratio of the 1*f*-WMS signal along the two lock-in amplifier axes and is therefore immune to any changes in *I*, and there is no gain variation in the signal processing as only the first harmonic signal is recovered. This new technique would therefore be advantageous for applied gas sensing applications, particularly for embedded systems in chemical species tomography.

Acknowledgment

The authors wish to thank Mr. S. Morris, Managerial, Professional and Specialist Staff, Gas Turbine Research Centre, Cardiff University, for his support in successfully running the combustion measurement tests.

References

[1] V. Ebert, K.-U. Pleban, and J. Wolfrum, "In-situ oxygen-monitoring using near-infrared diode lasers and wavelength modulation spectroscopy," in *Proc. Conf. Laser Appl. Chem. Environmental Anal.*, 1998, pp. 206–209.

[2] K. Duffin, A. J. McGettrick, W. Johnstone, G. Stewart, and D. G. Moodie, "Tunable diode-laser spectroscopy with wavelength modulation: A calibration-free approach to the recovery of absolute gas absorption line shapes," *J. Lightw. Technol.*, vol. 25, no. 10, pp. 3114–3125, Oct. 2007.

[3] A. J. McGettrick, K. Duffin, W. Johnstone, G. Stewart, and D. G. Moodie, "Tunable diode laser spectroscopy with wavelength modulation: A phasor decomposition method for calibration-free measurements of gas concentration and pressure," *J. Lightw. Technol.*, vol. 26, no. 4, pp. 432–440, Feb. 2008.

[4] G. B. Rieker, J. B. Jeffries, and R. K. Hanson, "Calibration-free wavelength-modulation spectroscopy for measurements of gas temperature and concentration in harsh environments," *Appl. Opt.*, vol. 48, no. 29, pp. 5546–5560, Oct. 2009. [Online]. Available: http://ao.osa.org/abstract.cfm?URI=ao-48-29-5546

[5] K. Sun, L. Tao, D. J. Miller, M. A. Khan, and M. A. Zondlo, "Inline multi-harmonic calibration method for open-path atmospheric ammonia measurements," *Appl. Phys. B*, vol. 110, no. 2, pp. 213–222, 2013. [Online]. Available: http://dx.doi.org/10.1007/s00340-012-5231-2

[6] Z. Qu, R. Ghorbani, D. Valiev, and F. M. Schmidt, "Calibration-free scanned wavelength modulation spectroscopy—Application to H_2O and temperature sensing in flames," *Opt. Exp.*, vol. 23, no. 12, pp. 16 492–16 499, Jun. 2015. [Online]. Available: http://www.opticsexpress.org/abstract.cfm?URI=oe-23-12-16492

[7] G. Stewart, W. Johnstone, J. R. P. Bain, K. Ruxton, and K. Duffin, "Recovery of absolute gas absorption line shapes using tunable diode laser spectroscopy with wavelength modulation—Part 1: Theoretical analysis," *J. Lightw. Technol.*, vol. 29, no. 6, pp. 811–821, Mar. 2011.

[8] J. R. P. Bain, W. Johnstone, K. Ruxton, G. Stewart, M. Lengden, and K. Duffin, "Recovery of absolute gas absorption line shapes using tunable diode laser spectroscopy with wavelength modulation—Part 2: Experimental investigation," *J. Lightw. Technol.*, vol. 29, no. 7, pp. 987–996, Apr. 2011.

[9] C. S. Goldenstein, C. L. Strand, I. A. Schultz, K. Sun, J. B. Jeffries, and R. K. Hanson, "Fitting of calibration-free scanned-wavelength-modulation spectroscopy spectra for determination of gas properties and absorption lineshapes," *Appl. Opt.*, vol. 53, no. 3, pp. 356–367, Jan. 2014. [Online]. Available: http://ao.osa.org/abstract.cfm?URI=ao-53-3-356

[10] K. Sun, X. Chao, R. Sur, C. S. Goldenstein, J. B. Jeffries, and R. K. Hanson, "Analysis of calibration-free wavelength-scanned wavelength modulation spectroscopy for practical gas sensing using tunable diode lasers," *Meas. Sci. Technol.*, vol. 24, no. 12, p. 125203, 2013. [Online]. Available: http://stacks.iop.org/0957-0233/24/i=12/a=125203

[11] J. Chen, A. Hangauer, R. Strzoda, and M.-C. Amann, "VCSEL-based calibration-free carbon monoxide sensor at 2.3 μm with in-line reference cell," *Appl. Phys. B*, vol. 102, no. 2, pp. 381–389, 2011. [Online]. Available: http://dx.doi.org/10.1007/s00340-010-4011-0

[12] A. Upadhyay and A. L. Chakraborty, "Calibration-free 2f WMS with in situ real-time laser characterization and 2f RAM nulling," *Opt. Lett.*, vol. 40, no. 17, pp. 4086–4089, Sep. 2015. [Online]. Available: http://ol.osa.org/abstract.cfm?URI=ol-40-17-4086

[13] A. Upadhyay, D. Wilson, M. Lengden, A. L. Chakraborty, G. Stewart, and W. Johnstone, "Calibration-free WMS using a cw-DFB-QCL, a VCSEL, and an edge-emitting DFB laser with in-situ real-time laser parameter characterization," *IEEE Photon. J.*, vol. 9, no. 2, Apr. 2017, Art. no. 6801217.

[14] H. McCann, P. Wright, and K. Daun, "Chemical species tomography," in *Industrial Tomography* (Woodhead Publishing Series in Electronic and Optical Materials), M. Wang, Ed., Cambridge, England: U.K.: Elsevier, 2015, ch. 5, pp. 135–174. [Online]. Available: http://www.sciencedirect.com/science/article/pii/B9781782421184000058

[15] P. Kluczynski, Å. M. Lindberg, and O. Axner, "Background signals in wavelength-modulation spectrometry with frequency-doubled diode-laser light. I. Theory," *Appl. Opt.*, vol. 40, no. 6, pp. 783–793, Feb. 2001. [Online]. Available: http://ao.osa.org/abstract.cfm?URI=ao-40-6-783

[16] W. Johnstone, A. J. McGettrick, K. Duffin, A. Cheung, and G. Stewart, "Tunable diode laser spectroscopy for industrial process applications: System characterization in conventional and new approaches," *IEEE Sensors J.*, vol. 8, no. 7, pp. 1079–1088, Jul. 2008.

[17] R. Bauer, G. Stewart, W. Johnstone, E. Boyd, and M. Lengden, "3D-printed miniature gas cell for photoacoustic spectroscopy of trace gases," *Opt. Lett.*, vol. 39, no. 16, pp. 4796–4799, Aug. 2014. [Online]. Available: http://ol.osa.org/abstract.cfm?URI=ol-39-16-4796